Available online at www.CivileJournal.org

Civil Engineering Journal

(E-ISSN: 2476-3055; ISSN: 2676-6957)

Vol. 10, No. 01, January, 2024

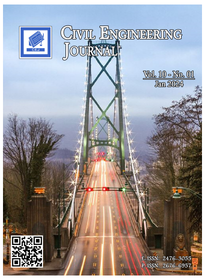

Prediction of the Dynamic Properties of Concrete Using Artificial Neural Networks

Amjad A. Yasin [1*]

[1] *Department of Civil Engineering, Faculty of Engineering Technology, Al-Balqa Applied University, 11134 Amman, Jordan.*

Received 11 September 2023; Revised 03 December 2023; Accepted 09 December 2023; Published 01 January 2024

Abstract

This study explores how dynamic characteristics of concrete, such as dynamic shear modulus, dynamic modulus of elasticity, and dynamic Poisson's ratio, affect stability and performance in civil engineering applications. Traditional testing procedures, which include the time-consuming and costly process of mixing and casting specimens, are both time-consuming and costly. The primary objective of this research is to improve efficiency by using Artificial Neural Networks (ANNs) and regression analysis to predict the dynamic properties of concrete, providing a machine-learning-based alternative to traditional experimental methodologies. A set of 72 concrete specimens was methodically built and evaluated, with compressive strengths of 50 MPa, aspect ratios ranging from 1 to 2.5, and an average density of 2400 kg/m^3. An input dataset and ANN targets were built using these samples. The ANN model, which used cutting-edge deep learning techniques, went through extensive training, validation, and testing, as well as statistical regression analysis. A comparison shows that the predicted dynamic modulus of elasticity and shear modulus using both ANN and regression approaches nearly match the experimental values, with a maximum error of 5%. Despite good forecasts for the dynamic Poisson's ratio, errors of up to 20% were detected on occasion, which were attributed to sample shape variations.

Keywords: Concrete; Dynamic properties; Artificial Neural Networks; Regression Analysis.

1. Introduction

Concrete, a key building material recognized for its strength and adaptability, is critical to contemporary society's infrastructure. Concrete's mechanical qualities, particularly its dynamic properties, are critical in determining the stability and performance of numerous civil engineering applications. The primary subject of much previous research on concrete was its dynamic compressive qualities, while tensile and Poisson's ratio properties were examined considerably less frequently [1]. During their service life, concrete buildings may be subjected to intensely dynamic loadings such as projectile impact and contact explosion, which would release a substantial amount of energy in a short period, emphasizing the need to investigate the dynamic characteristics of concrete [2]. Dynamic characteristics of concrete, such as dynamic shear modulus, dynamic modulus of elasticity, and dynamic Poisson's ratio, are important indications of how concrete buildings respond to external pressures like earthquakes and dynamic impacts. Estimating these qualities accurately is critical for ensuring the safety and lifespan of concrete structures. The dynamic characteristics of fine-grained concrete and foamed concrete were examined to assess these qualities and their usefulness in civil engineering construction [3, 4].

For testing these dynamic properties, the ultrasonic method is a beneficial, non-destructive tool. This approach gives critical insights into features such as dynamic shear modulus, dynamic modulus of elasticity, and dynamic Poisson's

* Corresponding author: dr.amjad.yassin@bau.edu.jo

http://dx.doi.org/10.28991/CEJ-2024-010-01-016

ratio by submitting concrete specimens to high-frequency ultrasonic pulses and studying their propagation through the material [5]. Ultrasonic pulse-echo testing usually necessitates the use of specialist equipment such as ultrasonic transducers, a pulse generator, and a receiver. The concrete specimen is tested by delivering high-frequency ultrasonic pulses into it. These pulses move through the material until they come into contact with an interface or a change in the substance's characteristics. The ultrasonic waves undergo some reflection back to the receiver when they contact limits, voids, or faults in the concrete. The time it takes for the wave to travel to and return from the border is measured. This duration, referred to as the "time-of-flight," is proportional to the depth and characteristics of the concrete. The ultrasonic wave velocity through concrete is intimately connected to its dynamic qualities. In testing, two types of waves are used: compressional (P-waves) and shear (S-waves). P-wave velocity is generally quicker and is proportional to the dynamic modulus of elasticity, whereas S-wave velocity is proportional to the shear modulus. The density and stiffness of the concrete affect the wave velocity. The obtained ultrasonic signals may be submitted to frequency analysis, allowing researchers to establish the concrete sample's resonance frequencies. These resonant frequencies give information on the specimen's inherent frequencies and mode shapes, which is critical to knowing its dynamic behavior. The observed velocities of the longitudinal and transverse waves are used to calculate the dynamic Poisson's ratio and the dynamic modulus of elasticity of concrete. These predicted values obtained could be compared to the theoretically estimated modulus of elasticity [6, 7].

Many earlier investigations on the dynamic characteristics of concrete have been conducted, including the dynamic compression mechanical properties of polyoxymethylene-fiber-reinforced concrete [8]. Dynamic properties test and constitutive study of lightweight aggregate concrete under uniaxial compression [9]. The correlation between static and dynamic modulus of elasticity on different concrete mixes [10] and the dynamic compressive properties of micro-concrete under different strain rates [11]. Dynamic deformation and fracturing properties of concrete under biaxial confinements [12], dynamic properties of lightweight aggregate and cellular lightweight concrete [13, 14], and dynamic properties of strain-hardening cementitious composite reinforced with basalt and steel fibers [15].

Historically, approaches to dynamic properties estimation depended on time-consuming and frequently expensive experimental testing, which may not be practicable in all circumstances. The demand for fast, cost-effective, and exact approaches to estimating these qualities has fueled computational intelligence research, notably Artificial Neural Networks (ANNs) [16, 17]. ANNs, a type of machine learning, have emerged as a potential method for learning from data and predicting complicated material behavior, providing an alternative to traditional experimental approaches. Because of their capacity to capture subtle non-linear correlations within data, they are well-suited to modeling the dynamic characteristics of concrete, which frequently display non-linear and time-dependent behavior. The use of Artificial Neural Networks (ANNs) in concrete technology and building has several applications and benefits. Concrete material qualities, such as compressive strength, tensile strength, and durability parameters, can be estimated using ANNs. ANNs may be used to provide more efficient and cost-effective alternatives to standard laboratory testing, allowing for faster property assessment [18-20].

ANNs can help optimize concrete mix designs by predicting the best combinations of elements (cement, aggregates, water, and admixtures) to meet specified performance criteria such as intended strength, workability, and durability [10, 21]. Also, it could be used to optimize the use of tuff stone content in lightweight concrete [15]. It is also used in concrete manufacturing to regulate quality. They are capable of monitoring and controlling the mixing and curing processes, guaranteeing that the concrete fulfills the needed standards and specifications [22]. Analyzing non-destructive testing data, such as ultrasonic testing and ground-penetrating radar, is conducted using ANNs. They aid in determining the state and structural integrity of concrete elements, as well as detecting flaws and abnormalities [7, 23]. The identification of symptoms of degradation or damage in concrete structures such as bridges and buildings over time is carried out using ANN for upkeep and safety [24, 25]. Concrete constructions subjected to environmental conditions such as corrosion, freeze-thaw cycles, and alkali-silica reactions are predicted using ANNs. These forecasts guide maintenance and repair efforts [26]. ANNs can help with concrete structure design optimization, such as identifying the best reinforcement scheme, slab thickness, or column dimensions for load-bearing capacity, safety, and cost-effectiveness [27, 28]. It is also used to study and forecast the complicated stress-strain behavior of restricted concrete columns under varied loading circumstances. ANNs examine experimental and simulation data to improve our knowledge of structural reactions, allowing us to build stronger and earthquake-resistant concrete structures [2]. Additionally, ANNs are utilized to estimate the dynamic parameter determination of concrete terrace walls with system identification [29]. Evaluate the dynamic properties of pre-treated rubberized concrete under incremental loading [30]. Evaluate the mechanical and dynamic properties of rubberized concrete [31], study the effect of loading rate on the dynamic properties of plastic concrete under triaxial loading [28], predict the residual flexural strength of fiber-reinforced concrete [32, 33], calculate the shear strength of corrosion-reinforced concrete beams [28], and validate and predict the physical properties of self-compacting concrete [34]. Predictive models based on ANNs are used to predict the ultimate conditions and stress-strain behavior of steel-confined ultra-high-performance concrete [35] and for the prediction of concrete properties [36].

Numerous experimental investigations have been conducted in the field of concrete engineering to anticipate the dynamic characteristics of concrete, providing significant insights into its behavior under varied settings. However, there is a significant gap in the investigation of using Artificial Neural Network (ANN) approaches to predict these characteristics. Despite the great number of traditional experimental investigations, the untapped potential of ANN in forecasting concrete dynamics is an uncharted field. Recognizing this gap, the current study seeks to address and bridge it by utilizing the power of ANN, thereby contributing to a more comprehensive understanding of concrete behavior and paving the way for innovative approaches in the field of structural engineering, which highlights the significance of this study.

The primary objectives of this research are to create and evaluate an effective approach for predicting the dynamic characteristics of concrete using Artificial Neural Networks (ANNs), such as dynamic shear modulus, dynamic modulus of elasticity, and dynamic Poisson's ratio. This may improve the accuracy and efficiency of property forecasts by using the power offered by machine learning as well as computational modeling, providing a viable alternative to standard experimental testing techniques. Furthermore, by offering a scalable and accessible approach for measuring the dynamic behavior of concrete materials, this research aims to contribute to the more general fields of civil engineering and structural dynamics. The study also aims to bridge the gap between the rising need for precise property estimates and the promise that ANNs provide in this respect. It is expected to provide insights that help improve the safety, dependability, and sustainability of concrete buildings in a variety of real-world applications through extensive testing and assessment.

The introductory section provides a thorough study of the most recent body of literature on the subject under consideration. The next section describes the materials and procedures used in this study, as well as the data sources used. The final portion expands on the findings and discussion, including the validation of the suggested model, a comparative analysis, and the implications of the results, all set against the background of earlier research attempts. The final section summarizes the study's findings and makes recommendations for future research in this field. This organized methodology allows a thorough examination of the research landscape, methodological complexities, findings, and implications, providing a well-rounded view of the study's contributions and future research options.

2. Materials and Experimental Program

2.1. Materials

The following ingredients and mix proportions were utilized in this study: Portland cement (Type I), coarse aggregate with a maximum size of 20 mm and a specific gravity of 2.65, natural sand with a specific gravity of 2.67 and a modulus of fineness of 2.77, micro silica of 2.17 specific gravity, superplasticizer with a specific gravity of 1.30, and fly ash (Class F) with a specific gravity of 2.30. Those mix proportions apply to typical-weight concrete with a target compressive strength of 50 MPa or more at 28 days. The ingredients were mixed in a 0.25 m^3 laboratory mixer. The mix proportions utilized in this experiment are given in Table 1. The density of all the produced concrete was around 2400 kg/m^3.

Table 1. Mix Proportions by Weight [7]

Coarse Aggregate: Fine Aggregate	1: 1.5
Cement: Fly Ash: Micro Silica	11.2: 2.16 :1
Cement +Fly Ash+ Micro Silica: Coarse Aggregate: Fine Aggregate	1: 1.92: 1.28
Water/ cement Ratio	0.30
Water/ (cement+ micro silica) Ratio	0.32

2.2. Experimental Program

The experimental program was created to investigate the dynamic physical characteristics of concrete and to assess the influence of concrete specimen size on these qualities. Prisms and cylinders with varied aspect ratios (L/d) (ranging from 1.0 to 2.5) were utilized as specimens. Table 2 shows the dimensions of the specimens utilized in this investigation.

Table 2. Specimens type, dimensions, and quantities [7]

Designation	Type and Dimensions (mm)	No. of Specimens
C150	Cube 150×150×150	12
C225	Prism 150×150×225	12
C300	Prism 150×150×300	12
C375	Prism 150x150×375	12
S200	Cylinders 100×200	12
S300	Cylinders 150×300	12

The careful use of specifically constructed molds for producing cubes, prisms, and cylinders for this study represented a varied spectrum of geometric shapes often found in building operations. After the concrete examples were cast, they underwent a rigorous demolding procedure to ensure structural integrity. Following that, the demolded specimens went through a drying phase at room temperature, precisely 20°C. This governed drying process is crucial for limiting moisture's possible influence on the following testing processes. The designed concrete specimens were next subjected to non-destructive testing using an ultrasonic pulse velocity tester according to the requirements provided in ASTM C587-09, as shown in Figure 1. The use of this testing apparatus corresponds to defined standards, ensuring consistency and accuracy in assessing the dynamic characteristics of concrete. The ASTM-compliant ultrasonic pulse velocity tester is a trustworthy instrument for evaluating the quality and structural features of concrete specimens, adding vital data to the whole study. The careful attention to each stage in this procedure, from specimen production to non-destructive testing, demonstrates a dedication to scientific rigor and supports the dependability of the obtained results in assessing the dynamic behavior of concrete.

Figure 1. Ultrasonic pulse velocity tester (ASTM C587-09) [37]

ASTM C597-09 is an ASTM International standard that describes how to use a resonant frequency apparatus to determine the dynamic modulus of elasticity and damping characteristics of concrete. The inherent frequencies of standard cubes and cylindrical concrete specimens exposed to vibrations are measured using this apparatus. ASTM C597-09 is used by inserting a tested specimen into the device and measuring resonance frequencies after applying force. The collected data gives insights into the dynamic behavior of concrete, assisting in the assessment of structural performance. The Results of the dynamic properties are given in Table 3.

Table 3. Experimental, ANN, and Regression Analysis Results of tested specimens

Designation	Strength (MPa)	L/D	Experimental			ANN Predicted			Regression Analysis		
			E_d (GPa)	G_d (GPa)	υ_d	E_d (GPa)	G_d (GPa)	υ_d	E_d (GPa)	G_d (GPa)	υ_d
C375	53	2.5	38.52	15.60	0.235	38.46	16.20	0.213	38.97	15.72	0.208
C375	53	2.5	38.50	15.59	0.234	38.46	16.20	0.213	38.97	15.72	0.208
C375	52	2.5	37.98	15.75	0.206	37.99	15.72	0.219	38.54	15.54	0.209
C375	52	2.5	37.98	15.73	0.205	37.99	15.72	0.219	38.54	15.54	0.209
C375	55	2.5	39.37	17.02	0.158	39.36	17.17	0.201	39.81	16.09	0.205
C375	55	2.5	39.37	17.00	0.156	39.36	17.17	0.201	39.81	16.09	0.205
C375	54	2.5	38.97	16.82	0.160	38.92	16.69	0.207	39.39	15.91	0.207
C375	54	2.5	38.97	16.80	0.159	38.92	16.69	0.207	39.39	15.91	0.207
C375	52	2.5	37.89	15.68	0.205	37.99	15.72	0.219	38.54	15.54	0.209
C375	52	2.5	37.89	15.70	0.207	37.99	15.72	0.219	38.54	15.54	0.209
C375	53	2.5	38.64	16.25	0.186	38.46	16.20	0.213	38.97	15.72	0.208
C375	53	2.5	38.64	16.29	0.188	38.46	16.20	0.213	38.97	15.72	0.208
C300	55	2.0	39.26	16.52	0.188	39.30	15.79	0.210	39.46	15.91	0.211
C300	55	2.0	39.26	16.52	0.188	39.30	15.79	0.210	39.46	15.91	0.211

C300	58	2.0	40.90	17.52	0.167	40.69	17.07	0.191	40.73	16.46	0.207
C300	58	2.0	40.90	17.52	0.167	40.69	17.07	0.191	40.73	16.46	0.207
C300	56	2.0	39.59	16.40	0.207	39.76	16.21	0.204	39.88	16.09	0.215
C300	56	2.0	39.59	16.40	0.207	39.76	16.21	0.204	39.88	16.09	0.215
C300	53	2.0	38.71	15.90	0.217	38.36	14.95	0.222	38.61	15.54	0.219
C300	53	2.0	38.71	15.90	0.217	38.36	14.95	0.222	38.61	15.54	0.219
C300	57	2.0	40.54	16.17	0.253	40.23	16.64	0.197	40.30	16.27	0.214
C300	57	2.0	40.54	16.17	0.253	40.23	16.64	0.197	40.30	16.27	0.214
C300	56	2.0	39.75	16.46	0.207	39.76	16.21	0.204	39.88	16.09	0.215
C300	56	2.0	39.75	16.46	0.207	39.76	16.21	0.204	39.88	16.09	0.215
C225	52	1.5	37.29	14.70	0.266	37.25	14.89	0.236	37.84	15.18	0.226
C225	52	1.5	37.31	14.72	0.267	37.25	14.89	0.236	37.84	15.18	0.226
C225	50	1.5	36.48	14.86	0.226	36.66	14.50	0.242	37.00	14.81	0.228
C225	52	1.5	36.50	14.88	0.228	37.25	14.89	0.236	37.84	15.18	0.226
C225	52	1.5	37.50	14.88	0.260	37.25	14.89	0.236	37.84	15.18	0.226
C225	53	1.5	37.54	14.90	0.263	37.55	15.10	0.234	38.26	15.36	0.225
C225	52	1.5	37.51	14.64	0.280	37.25	14.89	0.236	37.84	15.18	0.226
C225	53	1.5	37.55	14.68	0.282	37.55	15.10	0.234	38.26	15.36	0.225
C225	54	1.5	38.48	15.74	0.220	37.85	15.31	0.230	38.69	15.54	0.224
C225	54	1.5	38.52	15.78	0.224	37.85	15.31	0.230	38.69	15.54	0.224
C225	55	1.5	39.71	16.23	0.221	38.14	15.54	0.227	39.11	15.73	0.222
C225	55	1.5	39.75	16.227	0.225	38.14	15.54	0.227	39.11	15.73	0.222
C150	57	1.0	40.24	15.61	0.286	39.94	16.07	0.260	39.60	15.91	0.226
C150	57	1.0	40.28	15.65	0.288	39.94	16.07	0.260	39.60	15.91	0.226
C150	56	1.0	39.22	16.24	0.205	39.65	15.92	0.262	39.18	15.73	0.227
C150	56	1.0	39.26	16.28	0.209	39.65	15.92	0.262	39.18	15.73	0.227
C150	58	1.0	40.60	16.37	0.237	40.22	16.23	0.259	40.02	16.09	0.225
C150	58	1.0	40.64	16.41	0.241	40.22	16.23	0.259	40.02	16.09	0.225
C150	52	1.0	39.51	15.90	0.240	38.48	15.37	0.268	37.49	15.00	0.232
C150	53	1.0	39.55	15.94	0.244	38.77	15.50	0.266	37.91	15.18	0.231
C150	54	1.0	38.76	15.50	0.248	39.07	15.63	0.265	38.33	15.36	0.230
C150	54	1.0	38.80	15.52	0.252	39.07	15.63	0.265	38.33	15.36	0.230
C150	58	1.0	40.26	16.34	0.230	40.22	16.23	0.259	40.02	16.09	0.225
C150	59	1.0	40.30	16.38	0.232	40.50	16.39	0.257	40.45	16.28	0.224
S300	53	2.0	38.47	15.00	0.280	38.36	14.95	0.222	38.61	15.54	0.219
S300	54	2.0	38.49	15.04	0.284	38.83	15.37	0.216	39.04	15.72	0.218
S300	53	2.0	38.07	14.86	0.277	38.36	14.95	0.222	38.61	15.54	0.219
S300	52	2.0	38.11	14.90	0.281	37.88	14.54	0.228	38.19	15.36	0.220
S300	52	2.0	38.46	14.97	0.281	37.88	14.54	0.228	38.19	15.36	0.220
S300	53	2.0	38.50	14.01	0.284	38.36	14.95	0.222	38.61	15.54	0.219
S300	52	2.0	37.80	14.12	0.339	37.88	14.54	0.228	38.19	15.36	0.220
S300	52	2.0	37.82	14.11	0.341	37.88	14.54	0.228	38.19	15.36	0.220
S300	52	2.0	37.66	14.00	0.344	37.88	14.54	0.228	38.19	15.36	0.220
S300	52	2.0	37.70	14.00	0.348	37.88	14.54	0.228	38.19	15.36	0.220
S300	58	2.0	40.26	16.34	0.230	40.22	16.23	0.259	40.02	16.09	0.225
S300	59	2.0	40.30	16.38	0.232	40.50	16.39	0.257	40.45	16.28	0.224
S200	55	2.0	39.45	15.43	0.275	39.75	15.67	0.235	39.46	15.91	0.217
S200	55	2.0	39.49	15.47	0.279	39.75	15.67	0.235	39.46	15.91	0.217
S200	53	2.0	38.64	15.10	0.278	39.19	15.31	0.240	38.61	15.54	0.219
S200	52	2.0	38.68	15.12	0.281	38.91	15.15	0.242	38.19	15.36	0.220
S200	52	2.0	39.84	15.20	0.308	38.91	15.15	0.242	38.19	15.36	0.220
S200	55	2.0	39.88	15.22	0.312	39.75	15.67	0.235	39.46	15.91	0.217
S200	57	2.0	40.32	15.68	0.282	40.30	16.05	0.229	40.30	16.27	0.214
S200	57	2.0	40.36	15.72	0.286	40.30	16.05	0.229	40.30	16.27	0.214
S200	52	2.0	39.00	15.33	0.270	38.91	15.15	0.242	38.19	15.36	0.220
S200	52	2.0	39.04	15.37	0.272	38.91	15.15	0.242	38.19	15.36	0.220
S200	55	2.0	39.30	15.83	0.238	39.75	15.67	0.235	39.46	15.91	0.217
S200	56	2.0	39.32	15.87	0.242	40.03	15.85	0.232	39.88	16.09	0.215

3. Methodology

3.1. Artificial Neural Networks

Artificial Neural Networks (ANN) provide a rigorous mathematical framework that may be used for predictive modeling in a variety of experimental areas, including the evaluation of the dynamic properties of concrete. These networks, which are made up of linked neurons, have connections that are weighed and built in layered designs (as seen in Figure 2-a). Individual neurons in an ANN perform two important activities, as shown in Figure 2-b. To begin, these neurons are used to compute the total of the products produced from each input, together with the associated weight. The output is then generated using an activation function appropriate to the ANN layer. The output transformation is determined by several activation functions, such as linear, logsig, or tansig. The output of a linear activation function is the computed summation, but utilizing logsig or tansig functions requires applying the relevant mathematical functions (as shown in Figure 3) [19, 20].

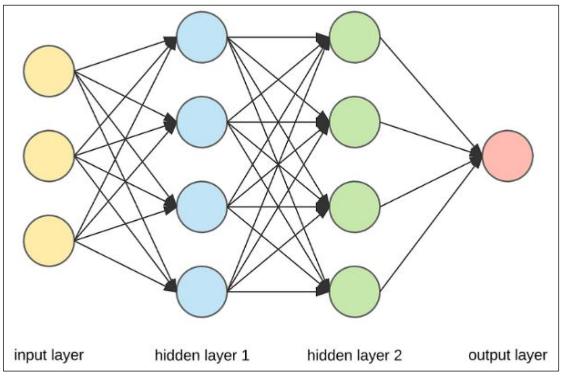

(a)

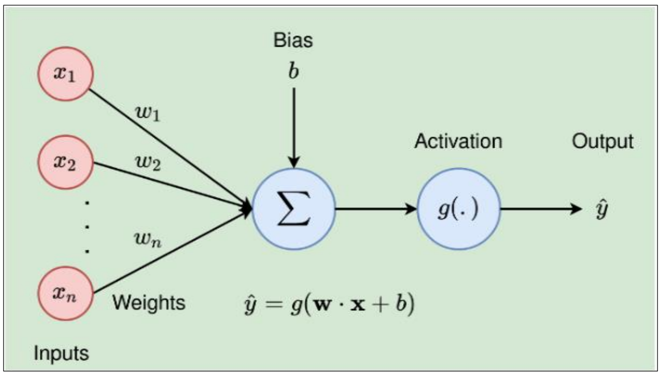

(b)

Figure 2. a- Neural Network Architecture, and b- ANN neuron operations

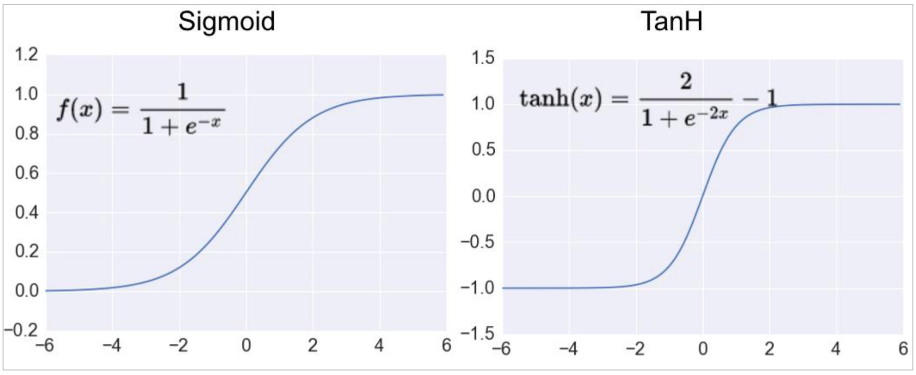

Figure 3. Activation functions of Logsig (left), and Tansig (right) [23]

3.2. Building an ANN Prediction Tool

Figure 4 gives a high-level overview of the primary procedures involved in creating an ANN model for use as a tool for prediction and illustrates a thorough visual depiction of the methodological processes used throughout this investigation. This diagram encapsulates the systematic and sequential techniques used to achieve the study objectives. Each step was thoroughly devised and carried out, taking into account the complexities of the experimental setup, data-gathering techniques, and analytical methodologies. The picture is a visual roadmap that explains the methodological framework that led to the investigation into the dynamic characteristics of concrete. It gives a thorough and informative portrayal of the research workflow, allowing for a more nuanced understanding of the activities necessary to guarantee the study's outcomes: rigor, correctness, and dependability.

The first step is to collect the necessary experimental data. It is necessary to arrange this data into a 2D matrix format, with each testing sample represented in its own column and the total sample count represented by the number of rows. A new matrix with 'm' columns is also required, where 'm' is the number of variables of interest to be examined. Following data collection, the data must be normalized. The purpose of this operation is to minimize the values of the incoming data to a predetermined range of 0 to 1. This is performed by dividing each data point by the greatest value associated with it. The next phase of this procedure is to build ANN's architectural design. During this phase, important structural decisions are made, such as defining the number of layers, assigning neurons to each layer, and selecting appropriate activation functions for each layer. Following architectural configuration, the important ANN parameters, most notably the Mean Squared Error (MSE), and the number of training cycles, are determined. The ANN model is then trained, and the gained MSE is assessed. If the MSE falls within the specified acceptable range, the trained artificial intelligence (ANN) model is kept for use as a forecasting tool in the future. If the MSE falls short of expectations, the fifth step is to launch an iterative method in which more training cycles are performed, with the results acting as inputs to the previous phase. The last stage entails an in-depth analysis of the MSE requirements. If these requirements are not satisfied, the ANN design must be refined methodically. Modifications to the number of layers, modifications to activation functions, or an increase in the number of the selected training cycles, followed by a training process repetition, are all conceivable.

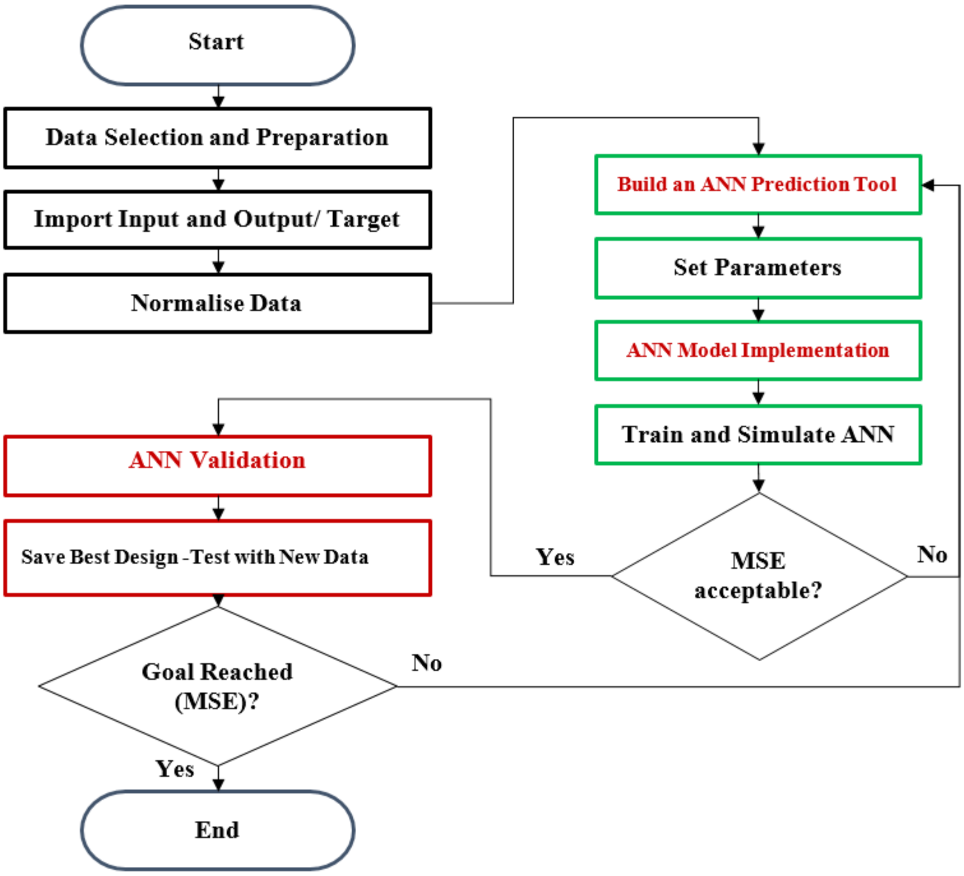

Figure 4. Methodology Flowchart of ANN predictor building, training, and validation

3.3. ANN Model Implementation Using MATLAB Software

The use of Artificial Neural Networks (ANN) to forecast the dynamic characteristics of concrete, especially inside the MATLAB software environment, represents a reliable and practical technique. MATLAB has a comprehensive range of tools and methods for creating, training, and analyzing neural network models. Engineers and researchers can use MATLAB's Neural Network Toolbox to create intricate ANN architectures, defining the network structure, number of layers, neurons, and activation functions necessary for predicting dynamic properties such as the dynamic modulus of elasticity, the dynamic shear modulus, and Poisson's ratio in concrete. The user-friendly interface of MATLAB allows for quick data preparation, training, and validation of ANN models utilizing a variety of datasets collected from experimental testing, non-destructive assessments, or simulations. Engineers may construct precise and trustworthy prediction models for concrete's dynamic characteristics by harnessing MATLAB's computational skills and specific neural network features, enabling improvements in the structural analysis and design of concrete structures. The findings of a study of 72 concrete specimens have been gathered. The usage of a MATLAB code dedicated to network construction, training, and testing benefited the development and evaluation of the ANN mode.

```
Data= data';

Data= data/2491.8;

In=data (1:6, :);

Tar= data (7:9, :);

Net=newcf (in, tar, [6 12], {'tansig','tansig'});
```

```
Net= init (net);
net.trainParam.goal=0;
net.trainParam.epochs=1000;
Net =train (net, in, tar);
y=sim (net, in);
```

Figure 5 illustrates the three stages of the ANN architecture employed. It consists of an input layer with 6 neurons, two hidden layers with 6 and 12 neurons, and an output layer with 3 neurons. The activation function inside the hidden layer is Logsig, but the activation function within the output layer is linear.

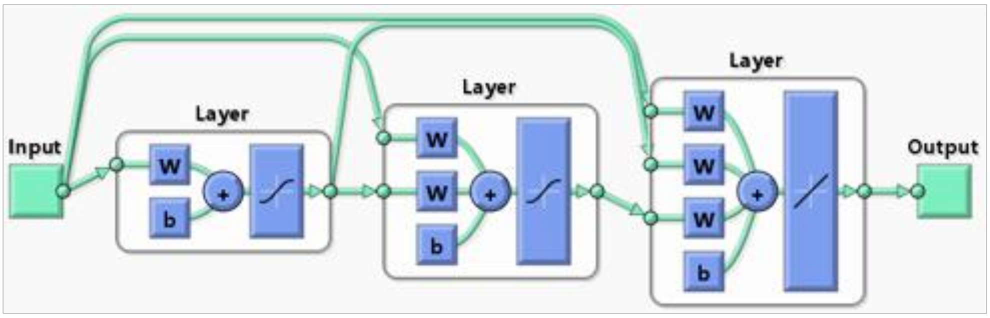

Figure 5. Used Artificial Neural Network

3.4. MATLAB and R-Programming Regression Analysis

Regression analysis is an effective statistical tool for examining relationships between two or more variables. Although regression analysis can be performed in a variety of methods, the common thread is an assessment of the influence of one or more independent variables on a dependent variable. Regression analysis was employed in this study to estimate the dynamic properties of concrete using MATLAB and R-programming tools. The following equations were obtained from the regression analysis:

$$E_d = -110.2111 + 0.4223\, f_c + 0.0521\, \gamma_c + 0.7018\, (L/D) \tag{1}$$

$$G_d = -55.8351 + 0.1829\, f_c + 0.0254\, \gamma_c + 0.3616\, (L/D) \tag{2}$$

$$\upsilon_d = 1.29 - 0.0013\, f_c + 0.000041\, \gamma_c + 0.0117 (L/D) \tag{3}$$

where E_d is Dynamic modulus of elasticity of concrete (GPa), G_d is Dynamic shear modulus of concrete (GPa), υ_d = Poisson's ratio of concrete, f_c is concrete compressive strength (MPa), γ_c *is concrete density* (kg/m^3), and *L/D* is Aspect ratio which is expressed as the length (*L*) to diameter (*D*) ratio in cylindrical samples of concrete or the height-to-width ratio in prismatic specimens.

4. Results and Discussion

The dataset provided in Table 3 was used to train the ANN. The ANN model worked brilliantly, lowering the Mean Squared Error (MSE) between predicted and target values. Figure 6 shows that the error was extremely low, registering a value of $1.22\text{x}10^{-8}$, suggesting that the expected outputs were near the planned targets. The ANN simulation results were deemed sufficient since, as shown in Figure 6, both the training and validation MSE curves exhibited a steady decline until approaching a stability point. The negligible distinction between the two curves demonstrated that no overfitting occurred, meaning that the number of training and validation specimens was carefully set for trustworthy predictions. Table 3 validates the predicted outputs' proximity to the desired values, as shown by the MSE in Figure 6.

The regression analysis was carried out using the MATLAB software, and the experimental data is presented in Table 3. This analytical approach was used to identify correlations and patterns in the dataset, and the resulting regression results have been thoroughly recorded and elegantly incorporated into the same table for easy reference. A detailed comparison study was conducted to guarantee a full assessment and validation of the prediction models. This entailed a thorough review of the results of experimental testing, Artificial Neural Network (ANN) modeling, and statistical regression analysis. Figures 7 to 9 carefully illustrate and graphically display the outcomes of this comparative investigation. These figures provide a clear and precise picture of the concordance or discrepancies between the experimental, ANN, and statistical regression analysis results. This comprehensive approach to comparative research enables a detailed understanding of each method's accuracy, dependability, and usefulness in forecasting the dynamic features of the concrete under examination.

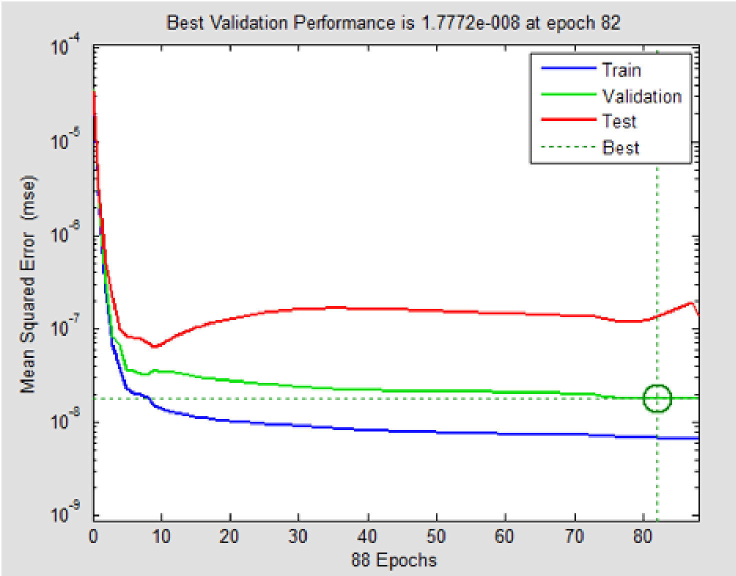

Figure 6. ANN performance indicator

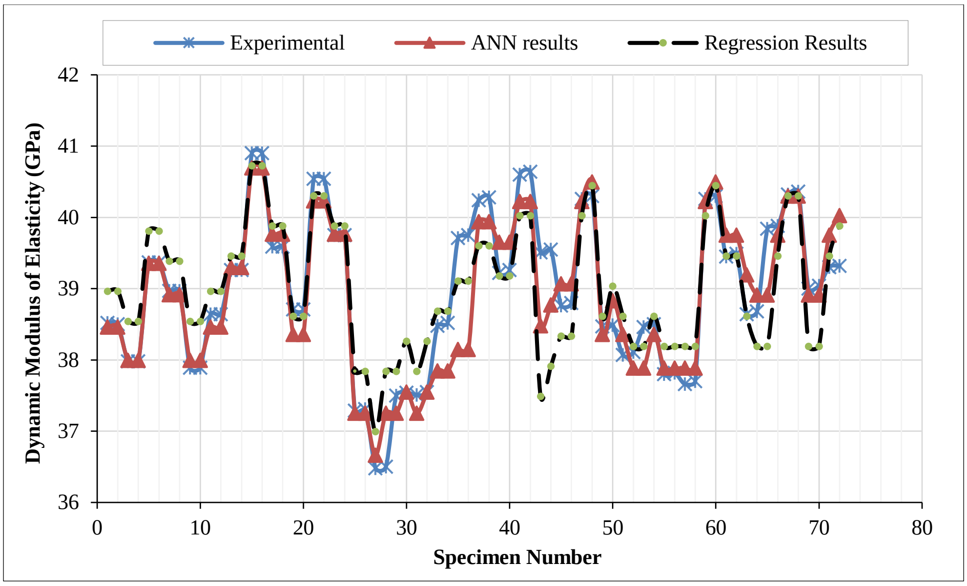

Figure 7. Dynamic Modulus of Elasticity for Test Specimens (Experimental, ANN, and Regression Analysis Results

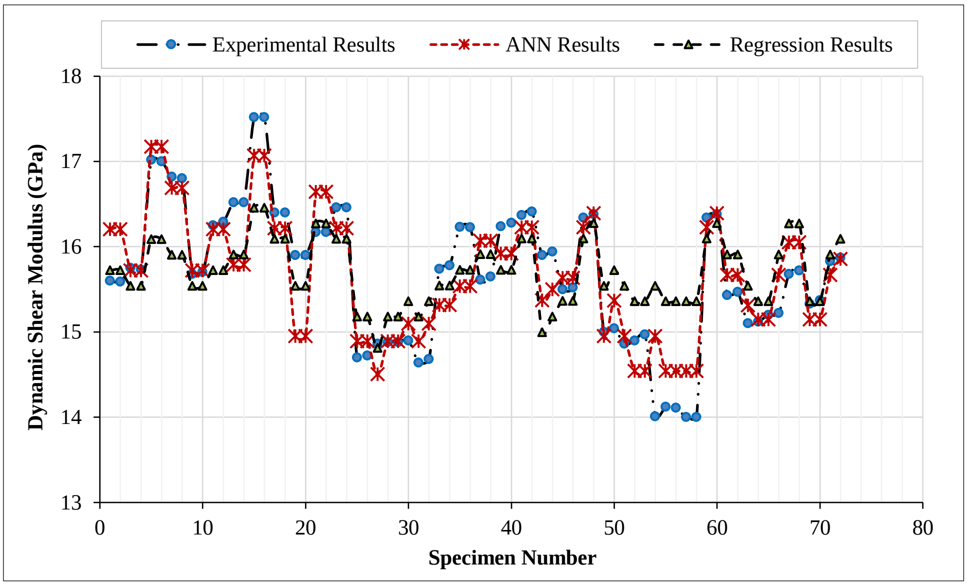

Figure 8. Dynamic Shear Modulus for Test Specimens (Experimental, ANN, and Regression Analysis Results)

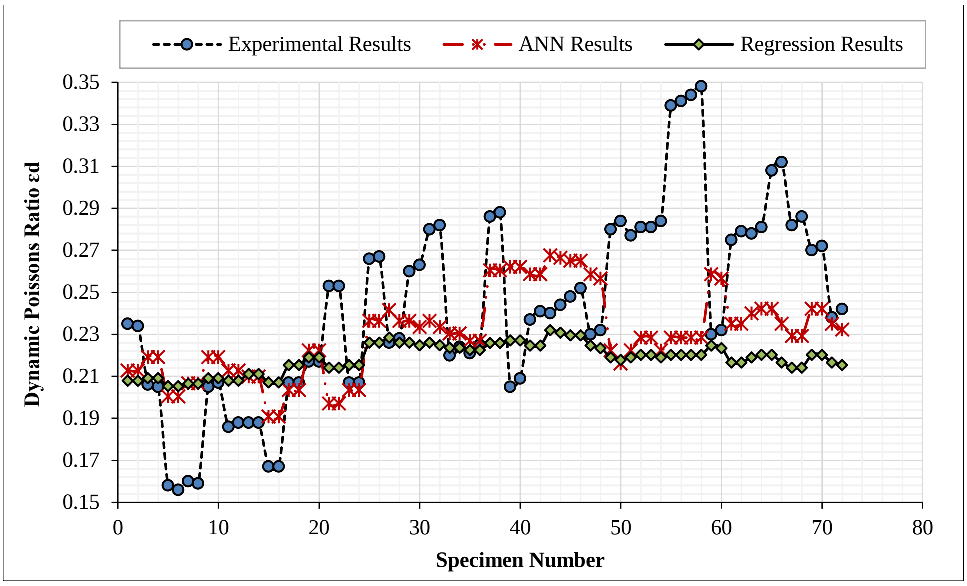

Figure 9. Dynamic Poisson's Ratio for Test Specimens (Experimental, ANN and Regression Analysis Results)

Figures 7 and 8 demonstrate a thorough visual presentation of the findings of the investigation comparing the expected dynamic modulus of elasticity and shear modulus. In this comparison investigation, both Artificial Neural Network (ANN) modeling and regression analysis approaches were used, and the results are surprisingly comparable with those obtained from experimental testing. The degree of agreement is strikingly high, with a maximum inaccuracy of 5% found. This tight agreement highlights the resilience and dependability of both ANN and regression analysis approaches in predicting the dynamic modulus of elasticity and concrete shear modulus. Figure 9 adds information on the dynamic Poisson's ratio, demonstrating a margin of error of about 20% for a certain number of specimens. This observed disparity, although existent, is restricted to specific occurrences and reflects the inherent difficulties associated with precisely estimating the dynamic Poisson's ratio, especially when sample variances or experimental subtleties are present. These figures' quiet insights contribute to a full understanding of the techniques' prediction capacities, prompting future modifications and considerations in the interpretation of dynamic characteristics in concrete.

The interpretation of this expected error is mainly due to the aspect ratio, which can affect the dynamic characteristics of concrete. According to research, the aspect ratio of cylindrical and prismatic specimens can impact dynamic qualities such as the dynamic modulus of elasticity and the dynamic Poisson's ratio. In general, as the aspect ratio increases, so does the dynamic modulus of elasticity. This decline is particularly noticeable at larger aspect ratios. This phenomenon happens to be due to the concrete specimen's diminished lateral confinement effect as the aspect ratio increases, influencing its dynamic behavior. Similarly, an increase in the aspect ratio might lead to a decrease in the value of the dynamic Poisson's ratio. Under dynamic loading circumstances, this reduction is frequently linked with a reduction in transverse elongation, leading to changes in the Poisson's ratio. It is crucial to note that these impacts might vary based on the concrete's unique composition, testing procedures, and ambient circumstances. The influence of the aspect ratio on dynamic characteristics is just one of numerous elements that can affect the performance of concrete under dynamic stress, and it is frequently investigated in conjunction with other parameters to understand its overall impact. Beyond mix design and aspect ratio, predicting dynamic characteristics in concrete requires taking into account many relevant aspects. Curing conditions, which include temperature and humidity throughout the curing phase, have a considerable influence on the dynamic behavior of concrete. Aggregate parameters such as compassion, size, shape, and gradation are critical in influencing the total dynamic response. The water-to-cement ratio, which is an important aspect of the strength and durability of concrete, can affect its dynamic properties. Chemical admixtures provide an additional degree of complexity by changing rheological and mechanical properties. Variations in dynamic characteristics are also caused by temperature changes during curing and testing, loading rate, concrete age, and the presence and layout of reinforcing components. Furthermore, the testing methodology used, such as ultrasonic or resonance testing, brings subtleties to the results. A comprehensive understanding of these many factors is critical for improving prediction models and ensuring correct evaluations of concrete's dynamic behavior in a variety of structural applications.

Regression analysis was conducted by MATLAB software. Figure 10 displays a thorough representation of projected values vs comparable experimental data. The observed distribution shows a random and symmetrical scattering of data points above and below the 45-degree diagonal line, indicating consistent variance across the dataset. The closeness of these data points to the diagonal line indicates that the model has a high level of goodness-of-fit. This finding emphasizes the model's accuracy in predicting values, as indicated by the model's little divergence from the idealized diagonal alignment. The total coefficient of determination (R-value) confirms the model's correctness, with a value of 0.99271. This strong R-value validates the suggested model's dependability and precision in predicting values with a high level of confidence.

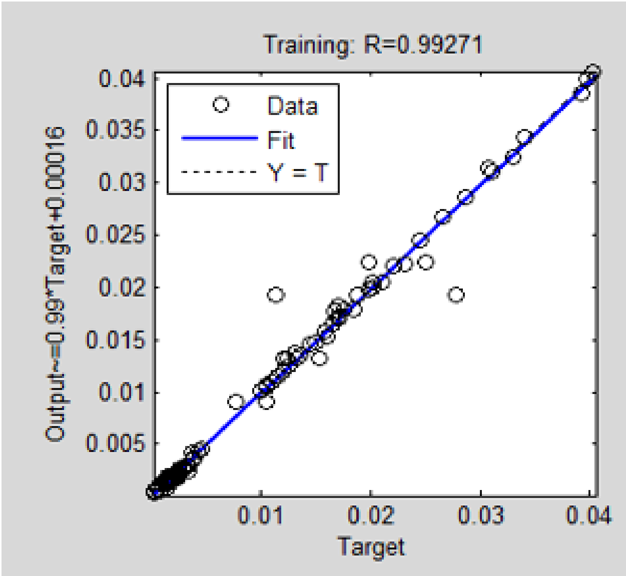

Figure 10. Regression predicted values vs. measured experimental results

5. Verification of the Proposed ANN Model

They developed an ANN model that was used to predict a unique dataset obtained from the available literature to demonstrate its usefulness. This dataset was divided into two distinct sets: The first set is for the use of concrete prisms with concrete strengths ranging from 20 to 45 MPa, an average concrete density of 2285 kg/m^3, and an aspect ratio of 7.85 to 15.93 [5]. The second set is for the use of standard concrete 15 cm cubes with concrete strengths ranging from 20 to 45 MPa, an aspect ratio of 1.0, and an average concrete density of 2430 kg/m^3 [20].

The dataset verification findings, extensively shown in Table 4, give a complete analysis of the efficacy and dependability of the prediction models used in this investigation. A careful examination of the validation results reveals that the dynamic characteristics of concrete could be predicted properly and dependably. Table 4 provides a thorough validation of the predictive models' performance, providing a quantitative assessment of their capacity to replicate and forecast the dynamic characteristics gained from experimental testing. This validation stage is critical for confirming the robustness of the created models, bolstering the credibility of the study's findings, and indicating the possibility of wider application in practical situations involving concrete materials and structural dynamics. The comprehensive display of these validation results in Table 4 contributes to the research methodology's transparency and accountability, allowing participants and researchers to assess the correctness and dependability of the prediction models used in the study.

Table 4. Experimental, ANN predicted, and regression analysis results of concrete specimens

Ref.	Unit Weight (kg/m^3)	Strength (MPa)	L/D	Experimental			ANN Predicted			Regression Analysis		
				E_d (GPa)	G_d (GPa)	υ_d	E_d (GPa)	G_d (GPa)	E_d (GPa)	E_d (GPa)	G_d (GPa)	υ_d
[14]	2273	22.6	15.15	29.2	11.9	0.167	28.90	11.60	0.280	28.39	11.51	0.154
	2265	22.6	14.91	28.7	11.6	0.168	28.60	11.66	0.263	27.80	11.22	0.160
	2314	22.6	15.60	28.9	11.7	0.188	28.86	11.71	0.328	30.84	12.72	0.132
	2284	22.6	15.93	28.8	11.7	0.181	29.39	11.75	0.310	29.51	12.07	0.140
	2276	22.6	15.27	28.8	11.7	0.180	28.91	11.65	0.283	28.63	11.63	0.151
	2299	22.6	7.85	29.5	11.8	0.177	12.22	14.88	0.260	24.62	9.53	0.228
[35]	2408.40	20.88	1.0	23.83	9.25	0.288	23.74	9.20	0.322	24.79	9.52	0.266
	2412.20	22.00	1.0	24.18	9.36	0.291	24.44	9.52	0.317	25.46	9.82	0.263
	2406.70	21.33	1.0	23.87	9.24	0.291	24.07	9.37	0.319	24.89	9.56	0.266
	2414.20	22.44	1.0	24.42	9.47	0.290	24.73	9.64	0.315	25.75	9.95	0.262
	2416.80	21.77	1.0	24.16	9.38	0.288	24.17	9.37	0.321	25.60	9.89	0.261
	2421.10	21.44	1.0	24.05	9.30	0.293	23.85	9.19	0.325	25.68	9.94	0.260
	2405.80	22.22	1.0	24.30	9.43	0.288	24.74	9.69	0.312	25.22	9.70	0.265
	2408.40	21.55	1.0	23.98	9.25	0.296	24.19	9.42	0.318	25.07	9.64	0.265

2416.20	21.77	1.0	24.03	9.29	0.294	24.19	9.38	0.321	25.57	9.88	0.262
2429.41	28.00	1.0	28.64	11.23	0.275	29.54	11.64	0.276	28.89	11.35	0.249
2440.03	26.66	1.0	28.06	10.97	0.279	27.90	10.92	0.294	28.87	11.38	0.246
2456.72	27.77	1.0	28.48	11.14	0.278	28.48	11.14	0.293	30.21	12.01	0.238
2425.01	28.44	1.0	28.70	11.21	0.280	30.06	11.87	0.270	28.84	11.32	0.250
2436.80	27.33	1.0	28.25	11.05	0.278	28.68	11.26	0.286	28.99	11.42	0.246
2418.03	28.22	1.0	28.58	11.18	0.278	30.02	11.86	0.268	28.39	11.11	0.253
2432.81	27.11	1.0	28.21	11.04	0.278	28.57	11.22	0.285	28.69	11.28	0.248
2446.42	28.88	1.0	28.88	11.31	0.277	29.91	11.79	0.278	30.15	11.95	0.241
2428.21	27.77	1.0	28.39	11.12	0.276	29.35	11.56	0.277	28.73	11.28	0.249
2435.63	31.77	1.0	33.03	13.22	0.249	32.44	12.96	0.259	30.80	12.20	0.242
2445.41	31.33	1.0	32.91	13.16	0.250	31.98	12.75	0.263	31.13	12.37	0.238
2454.80	30.22	1.0	32.69	13.10	0.248	30.89	12.24	0.272	31.15	12.41	0.236
2434.61	33.55	1.0	33.81	13.56	0.247	33.40	13.45	0.257	31.50	12.50	0.240
2448.53	32.00	1.0	33.60	13.53	0.242	32.38	12.95	0.262	31.57	12.57	0.236
2430.42	32.88	1.0	33.95	13.66	0.243	33.12	13.29	0.256	31.00	12.27	0.242
2459.30	30.66	1.0	32.75	13.12	0.248	31.14	12.36	0.272	31.57	12.60	0.233
2442.41	31.11	1.0	33.16	13.37	0.240	31.89	12.70	0.263	30.88	12.25	0.240
2436.22	34.44	1.0	34.13	13.68	0.247	33.78	13.65	0.258	31.96	12.71	0.238
2437.83	38.22	1.0	35.14	14.27	0.231	35.14	14.30	0.263	33.64	13.44	0.233
2456.81	39.77	1.0	35.70	14.40	0.240	35.82	14.62	0.264	35.29	14.20	0.223
2445.70	39.11	1.0	35.12	14.21	0.236	35.50	14.47	0.264	34.43	13.80	0.229
2435.71	40.66	1.0	35.70	14.38	0.241	35.92	14.58	0.265	34.56	13.83	0.231
2464.73	41.33	1.0	36.15	14.67	0.232	36.50	14.86	0.264	36.36	14.69	0.218
2446.44	39.77	1.0	35.55	14.33	0.240	35.74	14.55	0.265	34.75	13.94	0.228
2454.51	42.66	1.0	36.55	14.74	0.240	36.87	14.95	0.265	36.39	14.67	0.221
2463.70	41.77	1.0	36.14	14.67	0.232	36.66	14.91	0.264	36.49	14.74	0.218
2446.81	42.22	1.0	36.20	14.68	0.233	36.60	14.84	0.266	35.80	14.40	0.224
2456.68	45.11	1.0	38.58	15.59	0.237	37.82	15.23	0.264	37.53	15.18	0.217
2465.18	44.00	1.0	38.13	15.41	0.237	37.55	15.18	0.264	37.51	15.19	0.215
2462.22	44.88	1.0	38.35	15.51	0.236	37.84	15.25	0.264	37.73	15.28	0.215
2473.26	45.11	1.0	38.46	15.58	0.234	38.12	15.36	0.262	38.40	15.60	0.210
2491.85	43.77	1.0	38.16	15.45	0.235	37.81	15.33	0.260	38.80	15.83	0.204
2468.70	43.55	1.0	38.07	15.43	0.234	37.43	15.15	0.263	37.50	15.20	0.214
2490.74	43.11	1.0	37.82	15.32	0.234	37.51	15.24	0.261	38.46	15.68	0.205
2486.67	44.88	1.0	38.34	15.53	0.234	38.24	15.42	0.260	39.00	15.90	0.205
2464.81	44.44	1.0	38.33	15.53	0.234	37.71	15.22	0.264	37.67	15.26	0.214

Figures 11 and 12 show a comprehensive visual illustration of the comparison of the anticipated dynamic modulus of elasticity and shear modulus obtained by both Artificial Neural Network (ANN) modeling and regression analysis. These predictions are compared to the validation dataset's experimental testing outcomes. Surprisingly, the results of both ANN and regression analysis methodologies nearly match those of experimental testing, with a maximum error of 5%. This remarkably close agreement highlights the resilience and dependability of both modeling techniques in successfully forecasting the dynamic modulus of elasticity and shear modulus for concrete, as confirmed against a different dataset. Figure 13 looks into the dynamic Poisson's ratio, revealing a margin of error of roughly 20% for specimens with notable aspect ratio values. This observed disparity is consistent with the findings in the results and discussion sections, where the influence of aspect ratio on dynamic characteristics was carefully investigated. This sophisticated knowledge enables a contextual explanation of the observed mistakes in forecasting the dynamic Poisson's ratio, stressing the impact of certain geometric properties on the predictive models' performance. The clear illustration of these results in Figures 11, 12, and 13 adds depth to the study's conclusions, providing a nuanced view of the predictive capabilities of the approaches used across several elements of concrete's dynamic behavior.

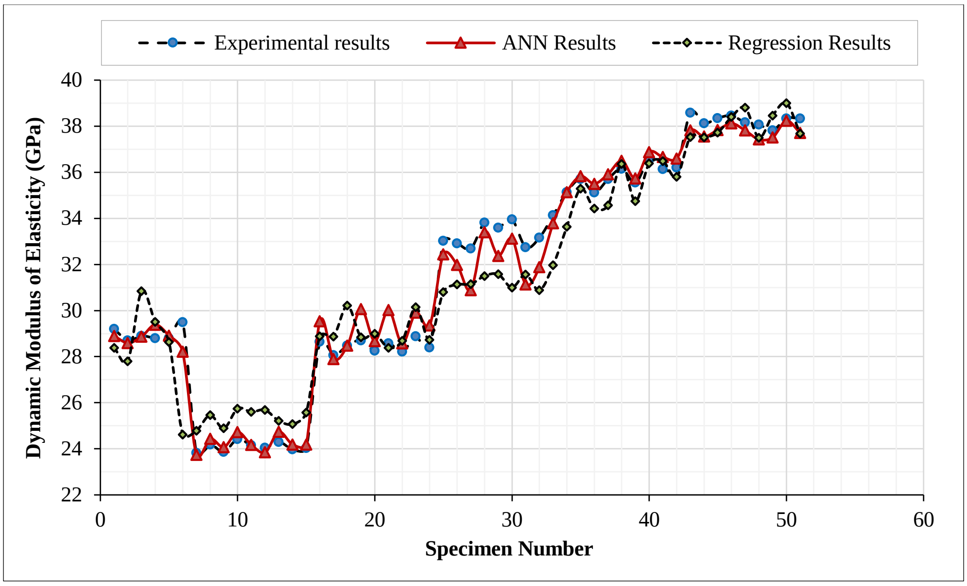

Figure 11. Dynamic Modulus of Elasticity for the Validation Datasets (Experimental, ANN and Regression Analysis Results)

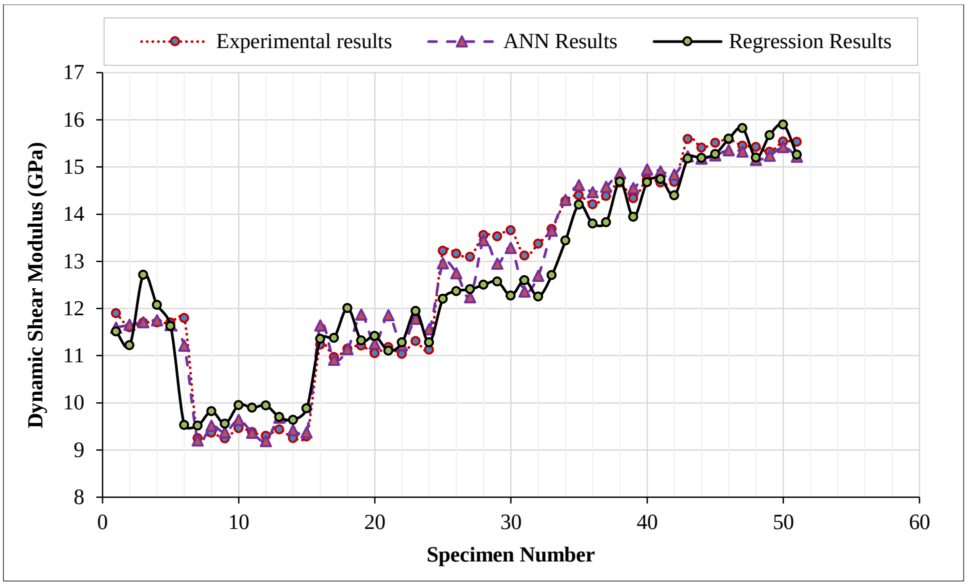

Figure 12. Dynamic Shear Modulus for Validation Datasets (Experimental, ANN, and Regression Analysis Results)

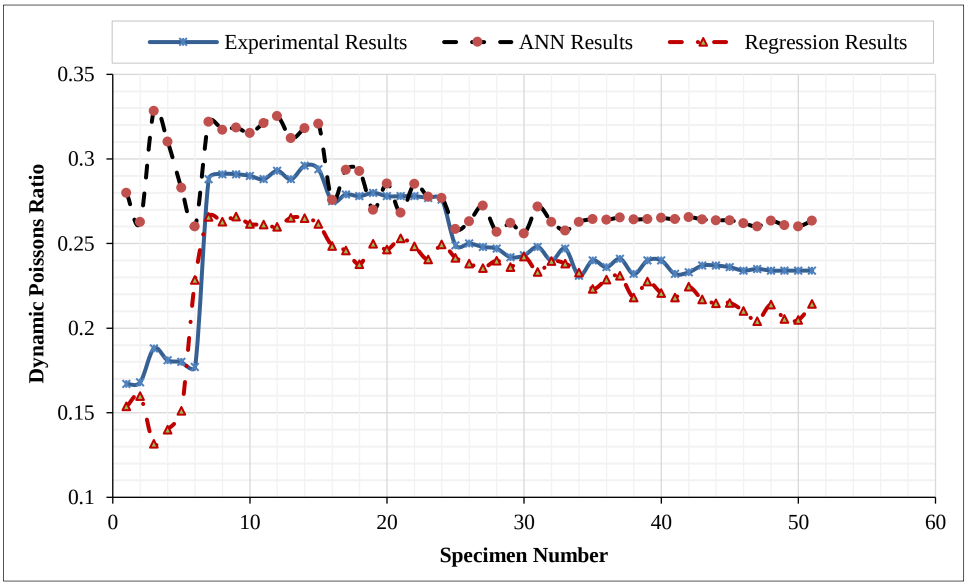

Figure 13. Dynamic Poisson's Ratio for Validation Datasets (Experimental, ANN, and Regression Analysis Results)

6. Conclusions

Throughout this study, an in-depth examination of the dynamic characteristics of concrete was undertaken utilizing a variety of approaches, including ultrasonic testing, Artificial Neural Networks (ANNs), and Regression Analysis. The research looked at the consequences of elements, including material properties and geometric characteristics, giving insight into their impact on the dynamic behavior of concrete. The research effort aims to improve the knowledge of how concrete responds to dynamic loads by using modern tools and methodologies, thereby considerably adding to civil engineering and construction. These detailed evaluations served as the foundation for generating significant findings critical to the advancement of concrete technology and structural dynamics, including the following:

- This study has successfully demonstrated the capability of non-destructive testing using an ultrasonic pulse velocity tester to provide accurate and acceptable estimates of concrete's dynamic mechanical properties. This approach proves to be highly reliable, offering dynamic property predictions that align well with those obtained in prior research investigations.
- There is a remarkable consistency between the experimental results and those obtained through ANN modeling and statistical regression analysis. The dynamic properties of concrete estimations from the ANN and regression analysis exhibited an error margin of less than 5%, but for a few specimens, it reached about 20%, especially for significant aspect ratios compared to the experimental findings. This exceptionally close agreement between experimental and computational methods underscores the accuracy and reliability of the developed ANN model, making it a powerful tool for estimating concrete's dynamic properties in real-world applications.
- The study not only validates the effectiveness of non-destructive testing for dynamic property estimation, but it also reveals nuances in the relationship between dynamic properties and aspect ratio in specific concrete scenarios, as evidenced by the comparison study of the Poisons ratio, which leads to an error of up to 20%.
- The results of this study offer various intriguing areas for future research in the field of concrete materials and structural dynamics. To begin with, incorporating sophisticated machine learning techniques other than ANNs, such as deep learning and convolutional neural networks (CNNs), gives an intriguing opportunity to enhance and broaden the scope of dynamic property estimation. Furthermore, examining broad datasets reflecting various concrete mix designs, ambient circumstances, and structural configurations can offer a more thorough knowledge of the subtle interactions between material attributes. Finally, the integration of multi-modal data sources, such as ultrasonic testing, acoustic emission, and vibration analysis, may allow for a more holistic approach to dynamic property estimation, improving the resilience and reliability of predictions.

7. Declarations

7.1. Data Availability Statement

The data presented in this study are available in the article.

7.2. Funding

The author received no financial support for the research, authorship, and/or publication of this article.

7.3. Acknowledgements

The author would like to acknowledge the technical support by the concrete laboratory in the Civil Engineering Department at the Faculty of Engineering Technology, Al-Balqa Applied University.

7.4. Conflicts of Interest

The author declares no conflict of interest.

8. References

[1] Kasopa, E., Chen, X., Yao, G., & Zhao, X. (2023). Dynamic Behavior of Concrete: A Review. International Journal for Research in Applied Science & Engineering Technology, 11(3), 294–304. doi:10.22214/ijraset.2023.49358.

[2] Cui, J., Guan, X., Shi, Y., & Li, Z. (2023). A high-fidelity constitutive model considering hydrostatic damage for predictions of high dynamic properties of concrete structures. Computers & Structures, 287(ue15). doi:10.1016/j.compstruc.2023.107115.

[3] Gonov, M. E., Balandin, V. V., Bragov, A. M., & Konstantinov, A. Y. (2023). Study of the Dynamic Properties of Reinforced Concrete under High-Speed Compression. Sixty Shades of Generalized Continua. Advanced Structured Materials, 170. Springer, Cham, Switzerland. doi:10.1007/978-3-031-26186-2_18.

[4] Ma, Z., Ma, C., Du, C., Zhang, S., Zhang, H., Zhang, X., Zhang, X., Wang, J., Tian, M., & Wang, Y. (2023). Research on dynamic mechanical properties of polypropylene fiber-modified rubber foamed concrete. Construction and Building Materials, 404, 10. doi:10.1016/j.conbuildmat.2023.133282.

[5] Ivanchev, I. (2022). Experimental determination of dynamic modulus of elasticity of concrete with ultrasonic pulse velocity method and ultrasonic pulse echo method. IOP Conference Series: Materials Science and Engineering, 1252(1), 012018. doi:10.1088/1757-899x/1252/1/012018.

[6] Wang, Z., Gao, Z., Wang, Y., Cao, Y., Wang, G., Liu, B., & Wang, Z. (2015). A new dynamic testing method for elastic, shear modulus and Poisson's ratio of concrete. Construction and Building Materials, 100, 129–135. doi:10.1016/j.conbuildmat.2015.09.060.

[7] Hajjeh, R. H., El-Sahawneh, E. I., Yasin, A. A., & Aw Wad, T. M. (2013). Determination of Dynamic Physical Properties of High Strength Concrete Using Ultrasonic Tester. International Journal of Multidisciplinary Research & Advances in Engineering, 5(II), 137–148.

[8] Guo, L., Guo, R., Yan, Y., Zhang, Y., Wang, Z., & Mu, Y. (2022). Dynamic Compression Mechanical Properties of Polyoxymethylene-Fiber-Reinforced Concrete. Materials, 15(21), 7784. doi:10.3390/ma15217784.

[9] Zhao, Z. (2021). Dynamic Properties Test and Constitutive Relation Study of Lightweight Aggregate Concrete under Uniaxial Compression. Advances in Materials Science and Engineering, 2021. doi:10.1155/2021/2678952.

[10] Trifone, L. (2017). A study of the correlation between static and dynamic modulus of elasticity on different concrete mixes. Master Thesis, West Virginia University, Morgantown, United States.

[11] Shen, D. J., & Lu, X. L. (2008). Experimental study on dynamic compressive properties of microconcrete under different strain rate. The 14th World Conference on Earthquake Engineering, 12-17 October, Beijing, China.

[12] Wang, H., Liu, K., & Zhang, Q. (2021). Dynamic deformation and fracturing properties of concrete under biaxial confinements. EPJ Web of Conferences, 250, 06008. doi:10.1051/epjconf/202125006008.

[13] Chen, H. J., Huang, C. H., & Tang, C. W. (2010). Dynamic properties of lightweight concrete beams made by sedimentary lightweight aggregate. Journal of Materials in Civil Engineering, 22(6), 599-606. doi:10.1061/(ASCE)MT.1943-5533.0000061.

[14] Wang, H. T., & Wang, L. C. (2013). Experimental study on static and dynamic mechanical properties of steel fiber reinforced lightweight aggregate concrete. Construction and Building Materials, 38, 1146-1151. doi:10.1016/j.conbuildmat.2012.09.016.

[15] Zhang, N., Zhou, J., & Ma, G. Wei. (2020). Dynamic Properties of Strain-Hardening Cementitious Composite Reinforced with Basalt and Steel Fibers. International Journal of Concrete Structures and Materials, 14(1), 44. doi:10.1186/s40069-020-00415-y.

[16] Gamil, Y. (2023). Machine learning in concrete technology: A review of current researches, trends, and applications. Frontiers in Built Environment, 9. doi:10.3389/fbuil.2023.1145591.

[17] Abdolrasol, M. G. M., Suhail Hussain, S. M., Ustun, T. S., Sarker, M. R., Hannan, M. A., Mohamed, R., Ali, J. A., Mekhilef, S., & Milad, A. (2021). Artificial neural networks based optimization techniques: A review. Electronics (Switzerland), 10(21), 2689. doi:10.3390/electronics10212689.

[18] Ramzi, S., Moradi, M. J., & Hajiloo, H. (2023). The Study of the Effects of Supplementary Cementitious Materials (SCMs) on Concrete Compressive Strength at High Temperatures Using Artificial Neural Network Model. Buildings, 13(5), 1337. doi:10.3390/buildings13051337.

[19] Yasin, A. A., Awwad, M. T., Malkawi, A. B., Maraqa, F. R., & Alomari, J. A. (2023). Optimization of Tuff Stones Content in Lightweight Concrete Using Artificial Neural Networks. Civil Engineering Journal (Iran), 9(11), 2823–2833. doi:10.28991/CEJ-2023-09-11-013.

[20] Pal, P. (2019). Dynamic poisson's ratio and modulus of elasticity of pozzolana Portland cement concrete. International Journal of Engineering and Technology Innovation, 9(2), 131-144.

[21] Habib, A., Yildirm, U., & Eren, O. (2020). Mechanical and dynamic properties of high strength concrete with well graded coarse and fine tire rubber. Construction and Building Materials, 246. doi:10.1016/j.conbuildmat.2020.118502.

[22] Al-Masoodi, A. H. H., Kawan, A., Kasmuri, M., Hamid, R., & Khan, M. N. N. (2016). Static and dynamic properties of concrete with different types and shapes of fibrous reinforcement. Construction and Building Materials, 104, 247–262. doi:10.1016/j.conbuildmat.2015.12.037.

[23] Abu-Faraj, M., Al-Hyari, A., & Alqadi, Z. (2022). Experimental Analysis of Methods Used to Solve Linear Regression Models. Computers, Materials & Continua, 72(3), 5699–5712. doi:10.32604/cmc.2022.027364.

[24] Mirbod, M., & Shoar, M. (2022). Intelligent Concrete Surface Cracks Detection using Computer Vision, Pattern Recognition, and Artificial Neural Networks. Procedia Computer Science, 217, 52–61. doi:10.1016/j.procs.2022.12.201.

[25] Miao, P., Yokota, H., & Zhang, Y. (2023). Deterioration prediction of existing concrete bridges using a LSTM recurrent neural network. Structure and Infrastructure Engineering, 19(4), 475–489. doi:10.1080/15732479.2021.1951778.

[26] Sun, B., Ping, Y., Zhu, Z., Jiang, Z., & Wu, N. (2020). Experimental Study on the Dynamic Mechanical Properties of Large-Diameter Mortar and Concrete Subjected to Cyclic Impact. Shock and Vibration, 2020, 9. doi:10.1155/2020/8861197.

[27] González-Pérez, C. A., & De-La-colina, J. (2022). Determination of Mass Properties in Floor Slabs from the Dynamic Response Using Artificial Neural Networks. Civil Engineering Journal (Iran), 8(8), 1549–1564. doi:10.28991/CEJ-2022-08-08-01.

[28] Asteris, P. G., & Nguyen, T.-A. (2022). Prediction of shear strength of corrosion reinforced concrete beams using Artificial Neural Network. Journal of Science and Transport Technology, 2(2), 1–12. doi:10.58845/jstt.utt.2022.en.2.2.1-12.

[29] T Tuhta, S. E. R. T. A. C., & Günday, F. (2020). Dynamic Parameters Determination of Concrete Terrace Wall with System Identification Using ANN. JournalNX- A Multidisciplinary Peer Reviewed Journal, 6(9), 194-202.

[30] Abdulabbas, Z. H., & Al Asadi, L. A. R. (2021). Calculating Dynamic Strengths of Concrete Subjected to Impact Load. Key Engineering Materials, 895, 12–19. doi:10.4028/www.scientific.net/kem.895.12.

[31] Habib, A., & Yildirim, U. (2022). Estimating mechanical and dynamic properties of rubberized concrete using machine learning techniques: a comprehensive study. Engineering Computations, 39(8), 3129–3178. doi:10.1108/ec-09-2021-0527.

[32] Wang, R., Cao, Z., Li, Y., Shi, Q., & Zhang, Y. (2022, January). Effect of loading rate on dynamic properties of plastic concrete under triaxial loading. MEMAT 2022; 2nd International Conference on Mechanical Engineering, Intelligent Manufacturing and Automation Technology, 7-9 January, 2022, Guilin, China.

[33] Congro, M., Monteiro, V. M. de A., Brandão, A. L. T., Santos, B. F. do., Roehl, D., & Silva, F. de A. (2021). Prediction of the residual flexural strength of fiber reinforced concrete using artificial neural networks. Construction and Building Materials, 303, 2021. doi:10.1016/j.conbuildmat.2021.124502.

[34] Thirumalai Raja, K., Jayanthi, N., Leta Tesfaye, J., Nagaprasad, N., Krishnaraj, R., & Kaushik, V. S. (2022). Using an Artificial Neural Network to Validate and Predict the Physical Properties of Self-Compacting Concrete. Advances in Materials Science and Engineering, 2022, 1–10. doi:10.1155/2022/1206512.

[35] Hiew, S. Y., Teoh, K. Bin, Raman, S. N., Kong, D., & Hafezolghorani, M. (2023). Prediction of ultimate conditions and stress–strain behaviour of steel-confined ultra-high-performance concrete using sequential deep feed-forward neural network modelling strategy. Engineering Structures, 277, 115447. doi:10.1016/j.engstruct.2022.115447.

[36] Abdulla, N. A. (2022). Application of artificial neural networks for prediction of concrete properties. Magazine of Civil Engineering, 110(2), 11007. doi:10.34910/MCE.110.7.

[37] ASTM C597-22. (2023). Standard Test Method for Pulse Velocity through Concrete. (2022). ASTM International, Pennsylvania, United States. doi:10.1520/C0597-22.